MOLECULAR AND CELLULAR BIOLOGY, Oct. 2003, p. 6982–6992 Vol. 23, No. 19
0270-7306/03/$08.00+0 DOI: 10.1128/MCB.23.19.6982–6992.2003

Rrp47p Is an Exosome-Associated Protein Required for the 3′ Processing of Stable RNAs

Philip Mitchell,[1]* Elisabeth Petfalski,[1] Rym Houalla,[1] Alexandre Podtelejnikov,[2] Matthias Mann,[2] and David Tollervey[1]

Wellcome Trust Centre for Cell Biology, Institute for Cell and Molecular Biology, University of Edinburgh, Edinburgh EH9 3JR, United Kingdom,[1] and Centre for Experimental Bioinformatics, University of Southern Denmark, DK-5230 Odense M, Denmark[2]

Received 7 April 2003/Returned for modification 23 May 2003/Accepted 3 July 2003

Related exosome complexes of 3′→5′ exonucleases are present in the nucleus and the cytoplasm. Purification of exosome complexes from whole-cell lysates identified a Mg^{2+}-labile factor present in substoichiometric amounts. This protein was identified as the nuclear protein Yhr081p, the homologue of human C1D, which we have designated Rrp47p (for rRNA processing). Immunoprecipitation of epitope-tagged Rrp47p confirmed its interaction with the exosome and revealed its association with Rrp6p, a 3′→5′ exonuclease specific to the nuclear exosome fraction. Northern analyses demonstrated that Rrp47p is required for the exosome-dependent processing of rRNA and small nucleolar RNA (snoRNA) precursors. Rrp47p also participates in the 3′ processing of U4 and U5 small nuclear RNAs (snRNAs). The defects in the processing of stable RNAs seen in *rrp47*-Δ strains closely resemble those of strains lacking Rrp6p. In contrast, Rrp47p is not required for the Rrp6p-dependent degradation of 3′-extended nuclear pre-mRNAs or the cytoplasmic 3′→5′ mRNA decay pathway. We propose that Rrp47p functions as a substrate-specific nuclear cofactor for exosome activity in the processing of stable RNAs.

The eukaryotic 18S, 5.8S, and 25S rRNAs (yeast nomenclature is given) are generated from a single large RNA polymerase I transcript by a series of endonucleolytic and exonucleolytic RNA processing reactions (reviewed in reference 39). The earliest detectable transcript in yeast, the 35S precursor rRNA (pre-rRNA), also undergoes extensive posttranscriptional modification involving predominantly pseudouridine formation and ribosyl-2′-O-methylation. These modifications are directed to specific nucleotides within the ~7-kb-long 35S pre-rRNA via complementary base-pairing mechanisms involving ~70 different small nucleolar RNAs (snoRNAs).

The snoRNAs can be divided into two major functional groups; the box C/D snoRNAs direct methylation of ribosyl-2′-hydroxyl groups, whereas the H/ACA snoRNAs direct the conversion of uridine to pseudouridine (for reviews, see references 4 and 21). Genes encoding snoRNAs have a varied organization, but in yeast and mammals all are transcribed by RNA polymerase II. Most yeast snoRNA genes are expressed as individual transcripts from their own promoters, whereas several are processed from common primary transcripts and a few are encoded within the introns of protein-coding genes. Gene clusters are the predominant organization of snoRNA genes in plants, whereas the majority of mammalian snoRNAs are intron encoded.

The synthesis of the mature 3′ ends of all characterized snoRNAs requires endonucleolytic cleavage of the transcript, followed by 3′→5′ exonucleolytic processing. Endonucleolytic cleavage is by Rnt1p, the yeast RNase III homologue, or by cleavage factor 1A (CF1A), which is also required for the 3′ end processing of mRNA transcripts (15). Maturation of intron-encoded snoRNAs involves linearization of the excised intron lariat, either by the debranching enzyme Dbr1p or endonucleolytic cleavage, followed by exonucleolytic processing (30, 31).

The 3′ processing of snoRNAs involves the exosome (1, 37), a complex of 9 to 10 distinct 3′→5′ exonucleases that functions in both RNA processing and degradation pathways. Nuclear and cytoplasmic forms of the exosome complex have been characterized that share 10 common components and differ by the presence of the RNase Rrp6p and the putative GTPase Ski7p, respectively (3). The 10 common components are all essential for cell viability. In contrast, *rrp6*-Δ mutants are viable but temperature-sensitive lethal (ts-lethal) and specifically impaired in exosome-mediated pathways in the nucleus (1, 8, 9, 19, 35, 37). In *rrp6*-Δ strains, most box C/D snoRNAs have short 3′ extensions, indicating a specific role for Rrp6p in the final trimming step. Longer, 3′-extended snoRNA precursors also accumulate in both *rrp6*-Δ mutants and in strains mutant for other exosome components and these species are polyadenylated by poly(A) polymerase.

The yeast spliceosomal snRNAs U1, U2, U4, and U5 are also transcribed by RNA polymerase II and are cleaved in their 3′ flanking regions by Rnt1p. In the case of U1, U4, and U5, it has been demonstrated that Rnt1p cleavage provides an entry site for 3′ exonucleolytic processing by the exosome (1, 37). However, snRNA synthesis is not blocked in strains mutant for either Rnt1p or components of the exosome complex, suggesting that alternative processing pathways exist.

The 3′-end processing of mRNAs typically involves the coordinated cleavage of the nascent transcript and polyadenyl-

* Corresponding author. Mailing address: Wellcome Trust Centre for Cell Biology, Institute for Cell and Molecular Biology, King's Buildings, University of Edinburgh, Edinburgh EH9 3JR, United Kingdom. Phone: (44) 0131-650-7081. Fax: (44) 0131-650-7040. E-mail: pmitch@holyrood.ed.ac.uk.

ation of the generated 3′ terminus. The cleavage and polyadenylation reaction is tightly coupled to transcription termination. In *rna14-1* mutants, which are defective in CF1A activity, cleavage is inefficient and readthrough transcripts are generated that extend several kilobases into downstream genes (7). These readthrough transcripts are rapidly processed by the nuclear exosome and then either polyadenylated or degraded by an Rrp6p-dependent mRNA surveillance mechanism (35).

The exosome was initially characterized during analyses of the pre-rRNA processing pathway. Mutation of exosome components inhibits the conversion of 7S pre-rRNA to 5.8S rRNA and the degradation of the 5′ external transcribed spacer (5′ETS) fragment, with the accumulation of heterogeneous populations of partially processed RNAs (1, 3, 12, 26). RNA analyses of *rrp6*-Δ mutants revealed a distinct defect in 7S pre-rRNA processing (9), with the accumulation of 5.8S rRNA species that are 3′ extended by ~30 nucleotides (nt). Like most mutations that inhibit the synthesis of 5.8S and 25S rRNA, exosome mutants also show indirect effects on early pre-rRNA cleavage events that are required for 18S rRNA synthesis (2, 43).

Genetic studies indicate that exosome function in vivo requires the activity of additional cofactors that are not found in exosome preparations or are present only at substoichiometric levels. All characterized nuclear functions of the exosome require the putative RNA helicase Mtr4p/Dob1p (12, 24), whereas exosome-mediated cytoplasmic mRNA turnover pathways are dependent upon Ski7p and the Ski complex, comprising the putative RNA helicase Ski2p and the proteins Ski3p and Ski8p (10, 20, 38).

Here we report that the *YHR081w* gene product is a novel exosome-associated factor that we designate Rrp47p. This protein was previously shown to be nuclear in a systematic localization study (22) (for an image, see http://ygac.med.yale.edu) and is homologous to the human nuclear protein C1D (14). Rrp47p and C1D are both implicated in DNA double-strand break repair (14, 41). We demonstrate that *rrp47*-Δ mutants are defective in the nuclear processing of pre-rRNA, snoRNAs, and snRNAs. In contrast, Rrp47p is not required for the exosome-mediated cytoplasmic 3′→5′ mRNA decay pathway or the nuclear degradation of 3′-extended readthrough transcripts generated in the *rna14-1* mutant. Rrp47p therefore exhibits characteristics of an exosome cofactor required specifically for the 3′ processing of stable RNAs.

MATERIALS AND METHODS

Strains. Yeast transformations were performed with plasmids or PCR-amplified DNA by using standard molecular biological techniques. Transformants were isolated by growth on selective media and integrants were screened by PCR directly on restreaked colonies. Strains were routinely grown in yeast extract-peptone-dextrose (YPD)-rich medium. The zz-Rrp44p strain (P203) was grown in rich medium containing galactose and sucrose as carbon sources. For the analysis of the *rna14-1 GAL::rrp41* mutant, the strain was pregrown in YPD medium for 24 h to deplete Rrp41p levels before transfer to 37°C.

Strains P203 (zz-Rrp44p), P414 (Rrp47p-zz), and YRH1 (Rrp6p-TAP) were generated by integration of PCR-amplified DNA by using plasmids pTL27 (23), pJE39 (a gift from J. Brown, University of Newcastle) and pBS1479 (32), respectively. The Rrp47p-zz allele was shown to be functional by growth rate assays and analyses of 5.8S rRNA species. The *rrp47*-Δ and *rna14-1 rrp47*-Δ mutants were generated by transferring the *rrp47*-Δ::Kan^r-null allele from genomic DNA of a strain (accession no. Y01909) obtained from EUROSCARF (University of Frankfurt, Frankfurt, Germany) into a haploid derivative of the wild-type strain BMA38 (5) and an *rna14-1* strain (35), respectively. The *rrp47*-Δ *rrp6*-Δ strain was generated by crossing the respective single mutant strains, sporulation, and selection for the auxotrophic markers.

Protein analyses. Crude cell extracts from zz-Rrp44p (P203), Rrp47p-zz (P414), Rrp44p-TAP (16), and Rrp6p-TAP (YRH1) strains were prepared by a glass bead extraction procedure in TMN-150 lysis buffer (50 mM Tris-HCl [pH 7.6], 5 mM $MgCl_2$, 150 mM NaCl, 0.1% NP-40). Immunoaffinity purification of exosome complexes on immunoglobulin G (IgG)-Sepharose, elution of retained proteins in TMN-150 containing an increasing gradient of $MgCl_2$, and matrix-assisted laser desorption ionization–nanoelectrospray MS analyses of gel-purified proteins were performed as previously described (3, 25, 34). Immunoprecipitates from strains expressing Rrp47p-zz were treated with RNase A (2 μg ml^{-1} [final concentration]) and incubated for 60 min on ice before a wash with 5 ml of TMN-150 buffer and subsequent digestion with tobacco etch virus (TEV) protease (Invitrogen). Polyclonal antisera were raised in rabbit against His_6-tagged fusion proteins expressed in *Escherichia coli* comprising full-length Rrp4p (26) and the N-terminal 222 residues of Rrp6p after purification from cell lysates by immobilized metal ion affinity chromatography on Ni^{2+}-nitrilotriacetic acid-agarose (Qiagen) and SDS-PAGE. Antisera were used at a dilution of 1:5,000 for Western analyses.

RNA analyses. RNA isolation, electrophoresis through acrylamide-urea or agarose-formaldehyde gels, Northern blot transfer, and hybridization with labeled oligonucleotides were performed as described previously (6). The following probes were used in the present study: 20S (oligonucleotide 2), GCTCTTT GCTCTTGCC; $27SA_2$ (oligonucleotide 3), TGTTACCTCTGGGCCC; 27S (oligonucleotide 6), AGATTAGCCGCAGTTGG; 25S (oligonucleotide 7), CT CCGCTTATTGATATGC; 18S (oligonucleotide 8), CATGGCTTAATCTTTG AGAC; 5.8S rRNA (oligonucleotide 17), GCGTTGTTCATCGATGC; 5.8S/ITS2 boundary (oligonucleotide 20), TGAGAAGGAAATGACGCT; 5′ETS (oligonucleotide 33), CGCTGCTCACCAATGG; U14 (oligonucleotide 202), TCACTCAGACATCCTAGG; U18-3′ (oligonucleotide 206), GCTCTGTGCT ATCGTC; U14-3′ (oligonucleotide 210), GTATACGATCACTCAGAC; U18 (oligonucleotide 215), ATATATTATCTGTCTCCTC; snR13 (oligonucleotide 227), CACCGTTACTGATTTGGC; snR44 (oligonucleotide 237), CATGGGATTAAA TATCCCGG; U4 (oligonucleotide 243), CCGTGCATAAGGAT; U5 (oligonucleotide 244), AATATGGCAAGCCC; U4-3′ (oligonucleotide 246), AAAGAA TGAATATCGGTAATG; SCR1 (oligonucleotide 250), AAGGACCCAGAAC TACCTTG; snR38 (oligonucleotide 255), GAGAGGTTACCTATTATTACCC ATTCAGACAGGGATAACTG; snR8 (oligonucleotide 269), GCATGTTTAA TATGTATCAT; ACT1 (oligonucleotide 400), TCTTGGTCTACCGACGATA GATGGGAAGACAGCA; CYH2 (oligonucleotide 405), GTGCTTTCTGTGC TTACCGATACGACCTTTACCG; and MFA2pG (oligonucleotide 487), ATA TTGATTAGATCAGGAATTCC.

RESULTS

Purification of exosome-associated factors. To identify novel exosome cofactors, cell lysate from a strain expressing an epitope-tagged form of the exosome component Rrp44p (zz-Rrp44p), which contains two copies of the "z" domain of protein A fused to the N terminus, was passed over an IgG-Sepharose column. After being washed, associated proteins were eluted in a gradient of 0 to 2 M $MgCl_2$, resolved by sodium dodecyl sulfate-polyacrylamide gel electrophoresis (SDS-PAGE), and identified by mass spectrometry (Fig. 1A).

In addition to Rrp6p (Fig. 1A, lanes 3 to 4), two polypeptides identified by mass spectrometry in the eluate fractions were recovered at substoichiometric levels, as judged by visual inspection of Coomassie-stained gels (Fig. 1A). A ~25-kDa protein that dissociated from zz-Rrp44p at ~0.2 to 0.4 M $MgCl_2$ (Fig. 1A, lanes 1 to 2) was identified as the product of the *YHR081w* gene. A similarly sized protein was observed in the equivalent eluate fractions from zz-Rrp4p retained material in our previous analyses (3) but not identified. We designated this protein Rrp47p on the basis of its role in rRNA processing (see below) and copurification with the exosome (which contains Rrp4p, Rrp40p-Rrp46p, and Rrp6p). An ~80-kDa protein that dissociated from zz-Rrp44p with the other

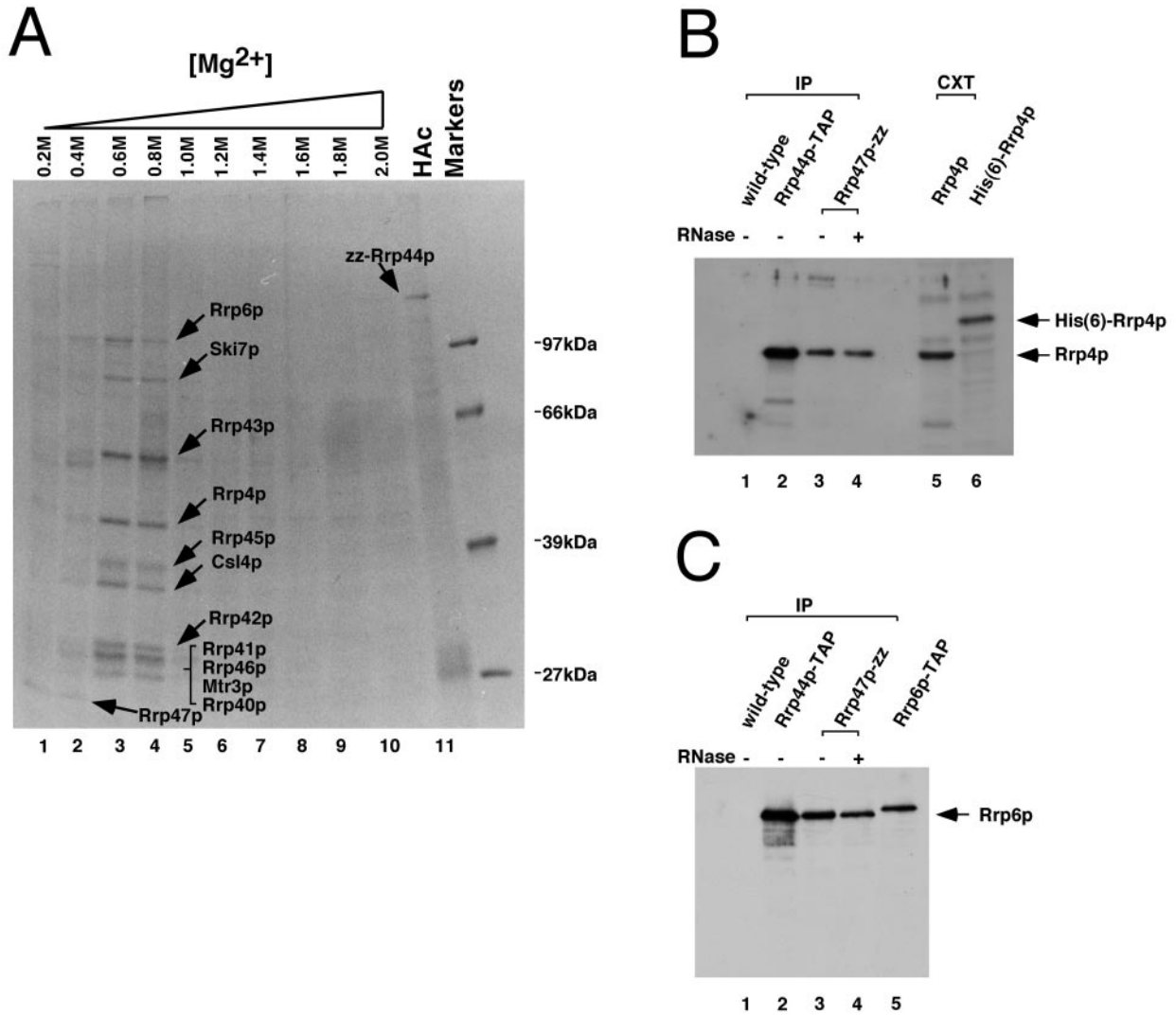

FIG. 1. Rrp47p is a novel exosome-associated factor. (A) Identification of Rrp44p-associated proteins. SDS-PAGE analysis of protein eluted from immunoprecipitated zz-Rrp44p was carried out. Lanes 1 to 10, linear 0 to 2 M $MgCl_2$ gradient in TMN-150 buffer; HAc lane, postgradient eluate in 0.5 M acetic acid. Proteins were visualized by staining with Coomassie G-250 and identified by mass spectrometry. Rrp47p was eluted in lanes 1 to 2 (~0.2 to 0.4 M $MgCl_2$). (B and C) Rrp47p is associated with Rrp4p and Rrp6p. Western blot analyses of immunoprecipitates from wild-type (lane 1), Rrp44p-TAP (lane 2), and Rrp47p-zz (lanes 3 to 4) strains, with antisera specific to Rrp4p (B) and Rrp6p (C) were done. Rrp47p-zz immunoprecipitates were eluted with or without prior digestion with RNase A. As controls for the specificity of the Rrp4p antiserum, cell extracts were loaded from strains expressing wild-type Rrp4p (B, lane 5) or epitope-tagged His (6)-Rrp4p (B, lane 6). Cleaved Rrp6p-TAP was included as a positive control for the Rrp6p Western analysis (C, lane 5). This protein is predicted to migrate slower than enodogenous Rrp6p in SDS-PAGE gels due to the presence of the calmodulin-binding domain.

exosome components (Fig. 1A, lanes 3 to 4) was identified as Ski7p (YOR076c), an exosome cofactor required for cytoplasmic 3′→5′ mRNA decay (38).

To confirm the interaction between Rrp47p and the exosome, a strain was constructed that expressed a C-terminal fusion protein linked by a TEV protease cleavage site (Rrp47p-zz). Lysate from the Rrp47p-zz strain was passed over an IgG-Sepharose column, and bound proteins were eluted by digestion with TEV protease. The eluate was assayed for the presence of Rrp4p by Western blot analyses, by using an anti-Rrp4p antiserum (Fig. 1B, lanes 3 to 4) (see Materials and Methods). As a positive control, lysate from a strain expressing TAP-tagged Rrp44p (Rrp44p-TAP) (16) was also analyzed (Fig. 1B, lane 2). Rrp4p was recovered from both the Rrp47p-zz and Rrp44p-TAP columns but was not detected in the eluate from the wild-type control strain (Fig. 1B, lane 1), confirming the interaction between Rrp47p and Rrp4p.

Previous analyses failed to detect any RNA species that copurified with the exosome complex (P. Mitchell and D. Tollervey, unpublished data). However, it remained formally possible that Rrp47p is associated with a ribonucleoprotein substrate of the exosome. Immunoprecipitated Rrp47p-zz was therefore treated with RNase A at 2 $\mu g\ ml^{-1}$ for 60 min prior to digestion with TEV protease. Rrp4p was detected at comparable levels with or without RNase treatment (Fig. 1B, lanes 3 and 4). The immunoprecipitation analyses shown were per-

formed in buffer containing 0.5 M NaCl, and the coimmunoprecipitation of Rrp47p-zz with Rrp4p therefore reflects a stable interaction.

The relative intensities of Rrp47p and the other exosome components observed in Coomassie blue-stained gels (Fig. 1A) suggests that Rrp47p is present in ~20% of the exosome complexes. Similarly, ~20% of the immunoprecipitated exosome complex is associated with Rrp6p (3). To assess whether Rrp47p and Rrp6p are associated with the same exosome fraction, the Rrp47p-zz immunoprecipitates were assayed for the presence of Rrp6p with an anti-Rrp6p antiserum (Fig. 1C, see Materials and Methods). Western blot analyses strongly decorated a single band of the predicted size in the Rrp47p-zz immunoprecipitate (Fig. 1C). This band was absent from total protein extracted from an *rrp6*-Δ strain (data not shown).

The *RRP47* gene is known to be nonessential for cell viability (17). To analyze the requirement for Rrp47p in exosome function, we generated an *rrp47*-Δ null allele (see Materials and Methods). The *rrp47*-Δ mutant exhibited a slow-growth phenotype at 25, 30, and 37°C, with a doubling time of 6.3 h at 37°C compared to 2.4 h for the isogenic wild-type strain (data not shown). Western blot analyses demonstrated that Rrp6p levels were not significantly altered in the *rrp47*-Δ mutant and that the coimmunoprecipitation of Rrp6p with an epitope-tagged Rrp4p fusion protein (zz-Rrp4p) was unaffected in the absence of Rrp47p (data not shown). We conclude that Rrp47p is not required for the expression of Rrp6p or its association with the exosome.

Rrp47p is required for normal pre-rRNA processing. Previous analyses revealed that exosome mutants are delayed in the early pre-rRNA cleavages at sites A_0, A_1, and A_2 (2, 43) (Fig. 2A). To address the role of Rrp47p in rRNA synthesis, RNA was isolated from the isogenic wild type, from *rrp47*-Δ and *rrp6*-Δ mutants, and from the ts-lethal *rrp4-1* mutant during growth at 30°C and after a 3 h shift to 37°C.

Large pre-rRNA processing intermediates were analyzed by Northern blot hybridization of RNA resolved in agarose-formaldehyde gels (Fig. 2). The *rrp47*-Δ mutant exhibited a mild accumulation of the 35S pre-rRNA, accompanied by an accumulation of the 23S and 21S RNAs (Fig. 2B) that are generated by cleavage at site A_3 in the absence of prior processing at sites A_0 to A_2 (18). These results indicate that early processing events at sites A_0, A_1, and A_2 are slowed in the *rrp47*-Δ mutant. The $27SA_2$ pre-rRNA also accumulated in the *rrp47*-Δ mutant (Fig. 2B). Primer extension (Fig. 2C) confirmed the accumulation of $27SA_2$ and showed mild depletion of $27SA_3$, as well as depletion of both $27SB_L$ and $27SB_S$ in the *rrp47*-Δ strain at 37°C. These results indicate that subsequent processing of the $27SA_2$ pre-rRNA was also impaired, as seen in previous analyses of other mutants of the exosome complex (2). The aberrant 17S′ species (Fig. 2B) extends from heterogeneous sites within the 18S rRNA to the 3′ end of 5.8S rRNA. This species has also been observed in exosome mutants (2) and is produced by a 5′→3′ degradation pathway when both processing in ITS1 and 3′ degradation are inhibited (40).

Ethidium bromide-stained acrylamide-urea gels of RNA from the *rrp47*-Δ mutant revealed a decrease in the level of 5.8S rRNA and the appearance of an aberrant RNA of ~200 nt (data not shown). The size and abundance of this RNA is similar to the 3′-extended "5.8S+30" rRNA that accumulates in strains lacking Rrp6p (3, 9). Northern blot hybridization with probes complementary to the mature 5.8S rRNA and to the 5.8S-ITS2 boundary hybridized to the same 5.8S+30 species in the *rrp47*-Δ and *rrp6*-Δ mutants (Fig. 3A). This 5.8S rRNA processing defect is distinct from that observed in strains mutant for "core" components of the exosome, such as Rrp4p, which is characterized by the accumulation of longer, 3′-extended 5.8S species (Fig. 3A) (26). Exosome mutants are also defective in the degradation of the 5′ETS fragment that is generated upon initial cleavage of the 35S pre-rRNA at site A_0 (1, 12). Hybridization with a probe complementary to a sequence 5′ of A_0 demonstrated that the 5′ETS fragment accumulated to a comparable level in the *rrp47*-Δ and *rrp6*-Δ mutants (Fig. 3B). Substantially stronger accumulation was seen in the *rrp4-1* mutant (Fig. 3B) and in strains depleted of other exosome components (1, 12).

Exosome mutants show a moderate inhibition of the endonucleolytic cleavages at sites A_0, A_1, and A_2. However, this phenotype is also seen for many other strains defective in 60S subunit synthesis (reviewed in reference 39) and is likely to be indirect. The defects seen in these early pre-rRNA processing steps in the absence of Rrp47p are similar to those of core exosome mutations. In contrast, the role of the exosome in the exonucleolytic processing of the 5.8S rRNA and in 5′ETS degradation are very likely to be direct and here the role of Rrp47p appears to resemble closely that of Rrp6p rather than the core exosome.

Rrp47p is required for snoRNA synthesis. Mutations in the exosome complex cause the accumulation of 3′-extended and polyadenylated snoRNA precursors. In *rrp6*-Δ mutants, but not in strains mutant for core exosome components, most box C/D snoRNAs also retain discrete 3′ extensions of ~3 nt (1, 37). To assay the role of Rrp47p in snoRNA synthesis, acrylamide gel-Northern blots were hybridized with probes specific for snR8 (box H/ACA) and snR13 (box C/D), which are transcribed from their own promoters, the dicistronic U14 snoRNA (box C/D) and the intron-encoded snoRNAs U18, snR38 (box C/D), and snR44 (box H/ACA) (Fig. 4).

As previously reported (1, 31), precursors to the intron-encoded snoRNAs were observed in the wild-type strain (labeled U18-3′, snR38-3′, and snR44-3′ in Fig. 4D to F) that have mature 5′ ends but are 3′ unprocessed. Similar 3′-extended precursors were also observed for snR8 and U14 (Fig. 4A and C). In the *rrp47*-Δ mutant, increased levels of these 3′-extended pre-snoRNAs and shorter 3′-extended species were observed for all snoRNAs tested. This indicates a requirement for Rrp47p in the 3′ processing of all classes of snoRNAs. A very similar pattern of 3′-extended snoRNA species was observed in the *rrp6*-Δ mutant, whereas a distinct pattern was observed in the *rrp4-1* mutant (Fig. 4). The 3′-extended snoRNA species observed in the *rrp6*-Δ mutant are polyadenylated (1, 37), yielding diffuse hybridization signals in the region of some bands (Fig. 4). The similar hybridization patterns observed in the *rrp47*-Δ and *rrp6*-Δ mutants strongly indicate that the extended species observed in the *rrp47*-Δ mutant are also polyadenylated.

Box C/D snoRNAs with short 3′ extensions of ~3 nt were observed in the *rrp6*-Δ mutant (indicated as "+3" species for snR13, U14, U18, and snR38 in Fig. 4) and these RNAs were also detected in the *rrp47*-Δ mutant. The levels of the U14+3

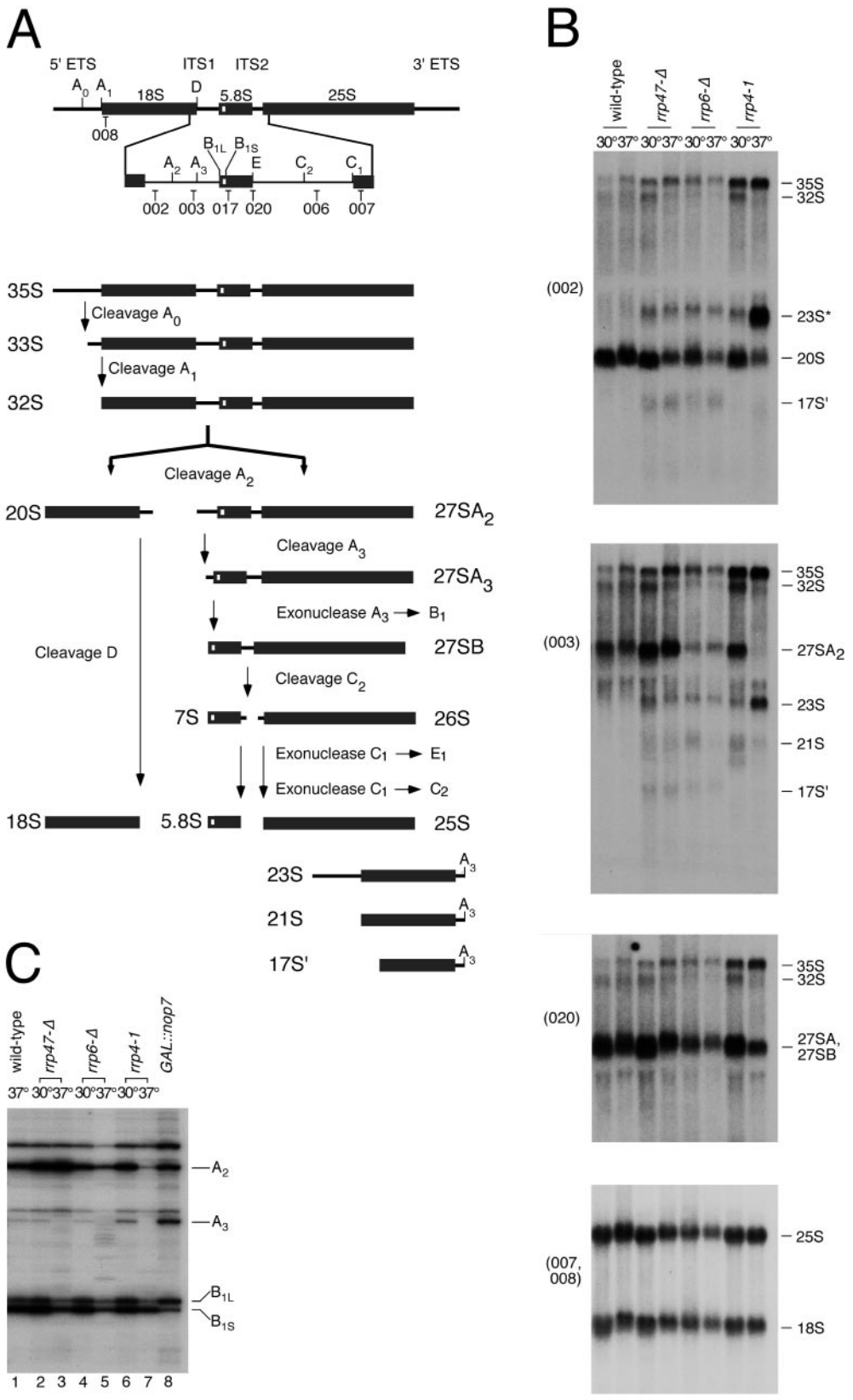

FIG. 2. Rrp47p is required for early pre-rRNA processing events. (A) Organization of the yeast pre-rRNA and processing pathway. The 18S, 5.8S, and 25S rRNAs are separated by internal transcribed spacers ITS1 and ITS2 and flanked by the external transcribed spacers 5′ETS and 3′ETS. Coding regions are indicated by thick bars; spacer regions are indicated by thin lines. Sites within the pre-rRNA complementary to probes used in the present study are indicated. Early cleavages at sites A_0, A_1, and A_2 generate the 20S and $27SA_2$ pre-rRNAs. The 20S pre-rRNA is processed to 18S rRNA by cleavage at site D. $27SA_2$ is processed in ITS1 and ITS2 to generate the 5.8S and 25S rRNAs. Two forms of 27SB, 7S, and 5.8S that differ by 7 nt at their 5′ ends (boxed) are generated by alternative processing pathways. The 23S and 21S pre-rRNAs arise through premature cleavage at site A_3. The 17S′ species results from 5′ degradation of pre-rRNA blocked for processing in ITS1. (B) Northern blot analyses

and snR38+3 species were reduced in the *rrp47*-Δ mutant compared to the levels observed in the *rrp6*-Δ mutant, whereas the U18+3 species appeared to be slightly shorter in the *rrp47*-Δ mutant after transfer to 37°C. Low levels of the snR13+3 species were observed in both the *rrp47*-Δ and *rrp6*-Δ mutants during growth at 30°C (Fig. 4B). In addition, a truncated fragment of snR13 ($snR13_T$) accumulated in the *rrp47*-Δ, *rrp6*-Δ, and *rrp4-1* mutants. This probably corresponds to the 5′-truncated snR13 species previously observed in *sen1-1* and *ssu72-2* mutants (13, 33). The reason for the appearance of this species is unclear but it strongly correlates with the generation or stabilization of snR13 readthrough transcripts, which are seen in several exosome mutant strains (A. Fatica and D. Tollervey, unpublished data).

We conclude that Rrp47p and Rrp6p play related roles in the initial processing of 3′-extended snoRNA precursors. However, the lack of Rrp47p has milder effects on the removal of the last few nucleotides than the absence of Rrp6p.

Rrp47p is required for normal synthesis of U4 and U5 snRNAs. The absence of Rrp6p or mutations in core components of the exosome complex also causes defects in the 3′ processing of snRNAs (1, 37). We therefore analyzed the levels of the U4 and U5 snRNAs and their processing intermediates in the *rrp47*-Δ mutant (Fig. 5).

Two 3′-extended pre-U4 species are detected in wild-type cells (1), denoted U4-3′I and U4-3′II (Fig. 5A). The U4-3′I intermediate has a short 3′ extension of ~6 nt, whereas the larger U4-3′II precursor is a pair of similarly sized RNAs ~140 nt longer than the mature U4 snRNA. Higher levels of the U4-3′II intermediate were observed in the *rrp47*-Δ mutant than in the wild-type strain (Fig. 5A). Shorter 3′-extended species were also observed in the *rrp47*-Δ mutant but not in the wild-type strain. A similar phenotype was observed for the *rrp6*-Δ and *rrp4-1* mutants (1, 37). No clear effect was observed on the levels of the U4-3′I or mature U4 snRNA in the *rrp47*-Δ mutant compared to the isogenic wild-type control strain.

In wild-type cells, mature U5 snRNA is present as a major, long form ($U5_L$) and a less-abundant short form ($U5_S$) that differ by ~35 nt at their 3′ ends. Precursor species with short extensions are observed in wild-type strains for both $U5_L$ and $U5_S$ (denoted $U5_L$-3′ and $U5_S$-3′, respectively), as well as a longer precursor denoted U5-3′I (Fig. 5B). The $U5_L$-3′, $U5_S$-3′, and U5-3′I precursors accumulated in the *rrp47*-Δ, *rrp6*-Δ, and *rrp4-1* mutants compared to the wild-type strain (Fig. 5B). Mutants in the exosome complex lead to increased levels of $U5_S$, while having little effect on the levels of $U5_L$ (1). Comparable levels of the minor $U5_S$ and major $U5_L$ snRNA were observed in the *rrp47*-Δ mutant, whereas the $U5_S$ form was the more abundant form in the *rrp6*-Δ and *rrp4-1* mutants (Fig. 5). Quantitative analyses revealed that the $U5_S/U5_L$ ratio increased in the *rrp47*-Δ, *rrp6*-Δ and *rrp4-1* mutants by 1.6-, 3.1-, and 2.9-fold, respectively, compared to the wild-type control.

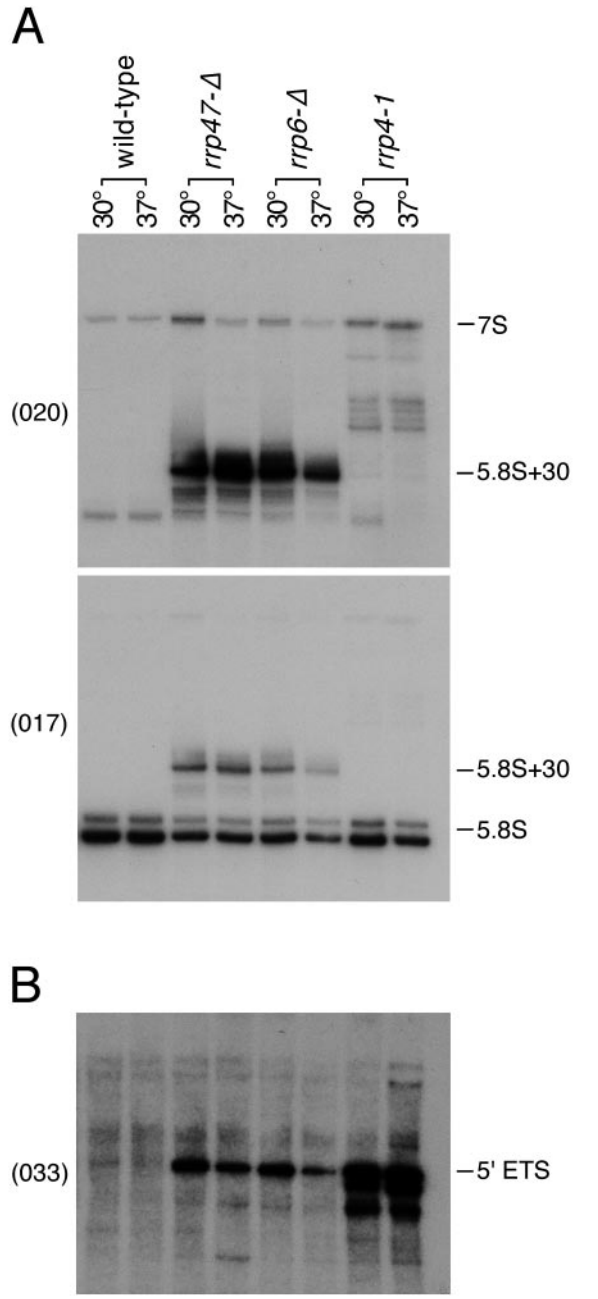

FIG. 3. Rrp47p is required for 7S pre-rRNA processing and 5′ETS degradation. (A) Northern blot analyses of 5.8S rRNA species in a wild-type strain and in exosome mutants. RNA was recovered from wild-type and mutant strains, as in Fig. 2. (Upper panel) Hybridization with a probe specific for 5.8S species extended into ITS2; (lower panel) hybridization with probe specific for the mature 5.8S rRNA. (B) Hybridization with a probe specific for the 5′ETS species. Probes used are indicated in parentheses to the left of each panel. The long and short forms of 5.8S rRNA are clearly resolved.

of pre-rRNAs from wild-type, *rrp47*-Δ, *rrp6*-Δ, and *rrp4-1* strains during growth at 30°C and after transfer to 37°C for 3 h. The probes used are given in brackets to the left of each panel; the species detected are indicated to the right (see panel A). The 23S* species detected with probe 002 is more abundant than 23S detected with probe 003 due to the limited 3′ degradation of 23S pre-rRNA in the *rrp4-1* mutant grown at 37°C. (C) Primer extension analyses of 27S pre-rRNAs with probe 006. Extension products corresponding to 27S species processed to sites A_2, A_3, B_{1L}, and B_{1S} are indicated. RNA from a *GAL::nop7* mutant grown in YPD medium for 24 h is included to provide a marker for the 5′ end of $27SA_3$ (29).

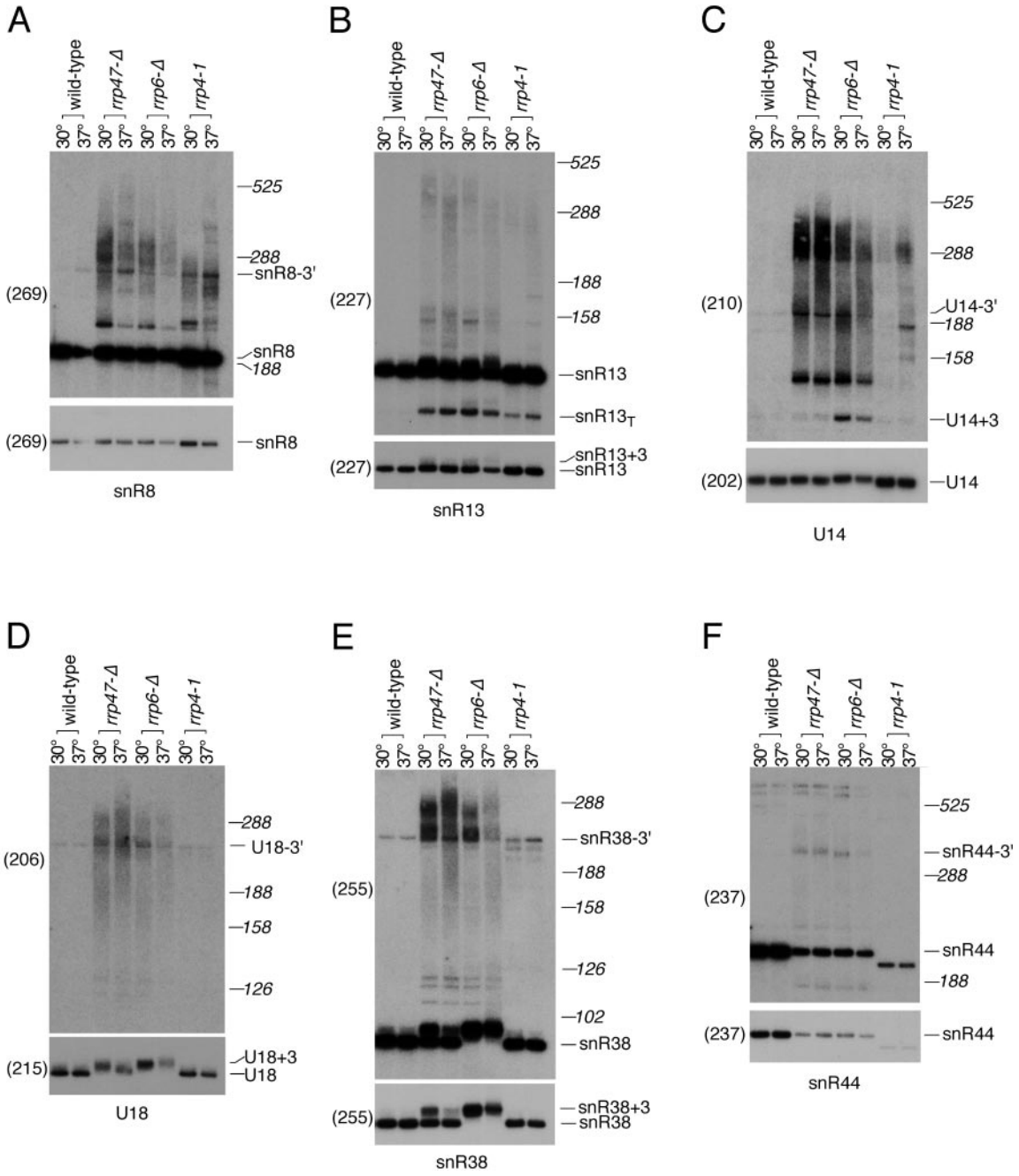

FIG. 4. Rrp47p is required for 3′ processing of snoRNAs. Northern blot analyses of snoRNA species were resolved in 6% (A and F) or 8% (B to E) acrylamide-urea gels. RNA was recovered from wild-type and mutant strains as in Fig. 2. (A) Hybridization with an snR8-specific probe; (B) hybridization with an snR13-specific probe (a truncated form [snR13$_T$] detected in the exosome mutants is indicated); (C) hybridization with a probe specific for 3′-extended U14 species; (D) hybridization with a probe specific for 3′-extended U18 species; (E) hybridization with an snR38-specific probe; (F) hybridization with an snR44-specific probe. Discrete, 3′-extended snoRNA precursors detected in the wild-type strain (snR8-3′, U14-3′, U18-3′, snR38-3′ and snR44-3′), and the snoRNAs with short, 3-nt extensions that are specifically detected in the *rrp47*-Δ and *rrp6*-Δ mutants (snR13+3, U14+3, U18+3, and snR38+3) are indicated. The lower panels show appropriate exposures of the hybridized blots to reveal clearly the mature snoRNAs. The probes used to detect snoRNA species are indicated in brackets to the left of each panel. The electrophoretic mobilities of *SCR1* (525 nt), 7S pre-rRNA (288 nt), 5.8S+30 (188 nt), 5.8S rRNA (158 nt), U14 (126 nt), and U18 (102 nt), determined by hybridization of the same filters, are indicated as size markers. The faster mobility of snR44 in the *rrp4-1* mutant is due to differences in the strain background.

Strains lacking Rrp47p therefore exhibit mild defects in U4 and U5 snRNA processing similar to those seen in strains lacking Rrp6p or mutant for core components of the exosome. We conclude that Rrp47p is required for the exosome-mediated 3′ processing of U4 and U5 snRNAs.

Analysis of the *rrp47*-Δ *rrp6*-Δ double mutant. To analyze further the functional relationship between Rrp47p and Rrp6p, we generated *rrp47*-Δ *rrp6*-Δ double mutants by genetic crossing. Sister strains from full tetrads showing a tetratype segregation for the *rrp47*-Δ and *rrp6*-Δ alleles were grown at

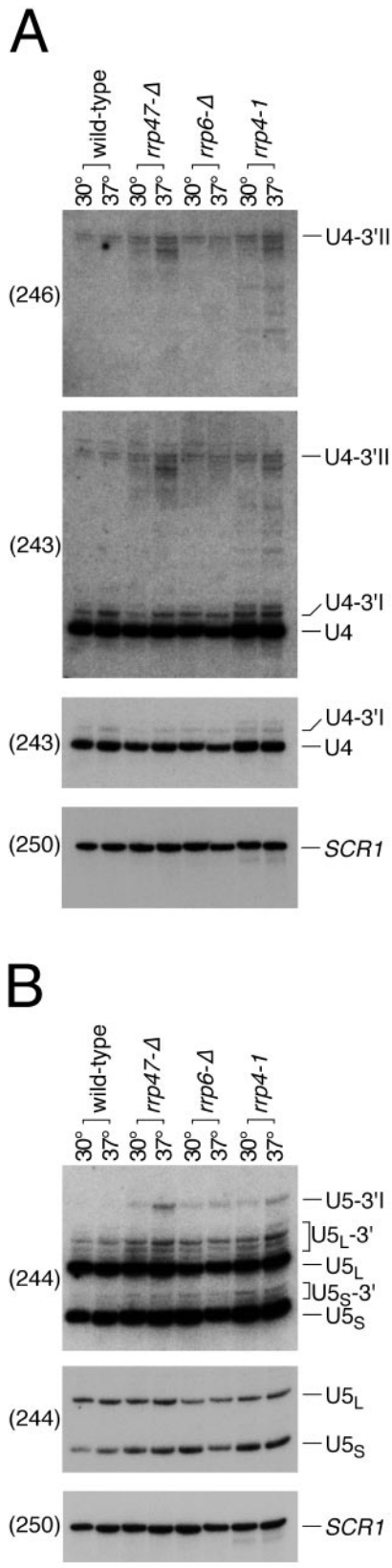

FIG. 5. Analysis of U4 and U5 snRNA species in the *rrp47*-Δ mutant. RNA was recovered from wild-type and mutant strains as in Fig. 2 and resolved in a 6% acrylamide-urea gel. (A) Analysis of U4 snRNA. (Upper panel) Hybridization with a probe specific for 3′-extended U4 snRNA species; (center panels) hybridization with a probe complementary to the mature U4 snRNA; (lower panel) control hybridization with a probe complementary to *SCR1*. (B) Analysis of U5 snRNA. Hybridization was performed with a probe complementary to the mature U5 snRNA. (Upper panel) long exposure (2 days) to reveal the 3′-extended U5 snRNA precursors; (middle panel) short exposure (3 h) to reveal the relative levels of the $U5_L$ and $U5_S$ snRNAs; (lower panel) hybridization with a probe complementary to *SCR1*. The probes used are indicated in brackets on the left of each panel.

30°C in YPD medium. The double-mutant strains were viable, with a growth rate comparable to that of the *rrp6*-Δ single mutant strain, indicating that the proteins do not have redundant functions.

This conclusion was supported by RNA analyses, which showed that the level of the 5.8S+30 intermediate in the *rrp47*-Δ *rrp6*-Δ double mutant was very similar to either single mutant (Fig. 6A). The 3′ processing of the U14 and snR38 snoRNAs in the *rrp47*-Δ *rrp6*-Δ double mutant resembled the *rrp6*-Δ single mutant rather than the *rrp47*-Δ single mutant, with a substantial accumulation of the short, 3′-extended species (Fig. 6B and C).

Recombinant Rrp6p has been demonstrated to have exonuclease activity (11), whereas sequence analyses do not suggest such an activity for Rrp47p. We therefore propose that Rrp47p is required for the activity of Rrp6p in 7S pre-rRNA processing and in the initial processing of snoRNA precursors. In contrast, Rrp47p promotes, but is not strictly required for, the Rrp6p-dependent final trimming of box C/D snoRNAs.

Rrp47p is not required for nuclear mRNA surveillance or cytoplasmic mRNA turnover. Rna14p is required for transcription termination of RNA polymerase II and the cotranscriptional cleavage and polyadenylation of mRNA transcripts. The absence of Rrp6p and the depletion of the core exosome component Rrp41p have distinct phenotypes in the mRNA surveillance pathways that degrade the readthrough transcripts generated in the ts-lethal *rna14-1* mutant (35). To address the role of Rrp47p in nuclear mRNA surveillance, we recovered RNA from *rna14-1*, *rna14-1 rrp47*-Δ, *rna14-1 rrp6*-Δ, and *rna14-1 GAL::rrp41* strains at time points after transfer to 37°C and then analyzed the *ACT1* and *CYH2* transcripts by hybridization of agarose gel-Northern blots (Fig. 7A).

Upon transfer to 37°C, the *ACT1* and *CYH2* mRNAs were rapidly depleted in the *rna14-1* mutant. Approximately normal length transcripts were stabilized in the *rna14-1 rrp6*-Δ mutant, whereas long extended transcripts accumulated in the *rna14-1 GAL::rrp41* mutant, as previously reported (35). In contrast, no mRNA stabilization was observed in the *rna14-1 rrp47*-Δ mutant and the *ACT1* and *CYH2* mRNAs were depleted upon transfer to 37°C with kinetics similar to the *rna14-1* single mutant. Consistent with the lack of suppression of *rna14-1* by the absence of Rrp47p, the *rna14-1 rrp6*-Δ mutant was viable at 37°C, whereas the *rna14-1 rrp47*-Δ mutant was not (Fig. 7B).

These data demonstrate that Rrp47p is not required for the nuclear, exosome-mediated initial degradation of the long readthrough transcripts generated in the *rna14-1* mutant or for the subsequent Rrp6p-dependent degradation of the truncated mRNAs.

Reporter constructs containing poly(G) tracts within the 3′

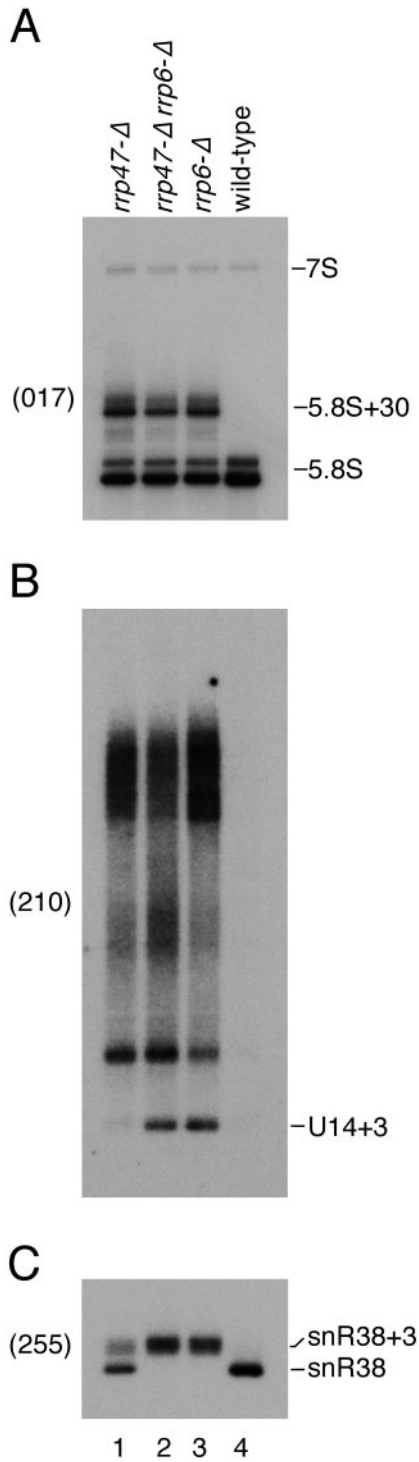

FIG. 6. Northern blot analyses of the *rrp47*-Δ *rrp6*-Δ double mutant. RNA from *rrp47*-Δ (lane 1), *rrp47*-Δ *rrp6*-Δ (lane 2), *rrp6*-Δ (lane 3), and wild-type (lane 4) sister strains grown at 30°C were resolved through an 8% acrylamide gel, transferred, and hybridized with probes specific for mature 5.8S rRNA (A), U14 3′-extended species (B), and mature snR38 (C). The probes used are indicated in brackets to the left of each panel.

untranslated region have been extensively used to trap and analyze intermediates in the exonucleolytic decay of cytoplasmic mRNA (reviewed in reference 36). In mutants of the exosome that are defective in cytoplasmic 3′→5′ mRNA decay, the turnover of the poly(G)→3′ end fragment of the *MFA2pG* reporter transcript is impeded compared to wild-type strains and shorter degradation intermediates accumulate (20). Constructs encoding the *MFA2pG* transcript were transformed into isogenic wild-type and *rrp47*-Δ strains, as well as a *ski7*-Δ mutant that is specifically defective for cytoplasmic mRNA decay. RNA recovered from the transformants was resolved in 8% polyacrylamide-urea gels and analyzed by Northern hybridization by using a probe complementary to the 3′ end of the poly(G) cassette. Degradation intermediates from the poly(G)→3′ fragment were observed in the *ski7*-Δ mutant but not in the *rrp47*-Δ mutant or the wild-type strain (Fig. 7C). This result demonstrates that Rrp47p is not required for the exosome-mediated cytoplasmic 3′→5′ decay pathway.

DISCUSSION

The exosome complex functions in a wide range of RNA processing and degradation pathways. It remains largely unclear how different classes of exosome substrates are initially identified and subsequently targeted to the very distinct fates of either accurate 3′ end processing or rapid and complete degradation. This differentiation is likely to be largely dependent upon additional cofactors that are predicted to be present at substoichiometric levels in exosome preparations and may be only weakly associated with the complex. We used a one-step immunoaffinity chromatography procedure coupled with elution of retained proteins in an increasing $MgCl_2$ concentration gradient to identify substoichiometric proteins associated with the exosome component Rrp44p. This allowed the identification of a novel exosome cofactor, Rrp47p. The association of Rrp47p with the exosome was insensitive to RNase treatment and therefore probably reflects a direct interaction. The substoichiometric levels of Rrp47p in exosome preparations and its electrophoretic mobility, which is similar to that of the five smallest core exosome components, presumably precluded its identification in previous analyses. Rrp47p was previously shown to be localized to the nucleus (22), suggesting that it associates with only the nuclear exosome. Consistent with this finding, Rrp47p was not required for cytoplasmic mRNA turnover. The nuclear-specific exosome component Rrp6p was efficiently coprecipitated with epitope-tagged Rrp47p, indicating that they are components of the same complex. A genome-wide analysis of protein complexes in yeast identified Rrp47p in the immunoprecipitates of the exosome components Rrp44p and Rrp46p (16). It should, however, be noted that the product of the *YIR035c* gene was also identified in association with exosome components in the same study, whereas a deletion mutant showed no defect in pre-rRNA or snoRNA processing or in cytoplasmic 3′→5′ mRNA decay (P. Mitchell, unpublished observations).

The RNA processing defects in the *rrp47*-Δ mutant resembled those previously observed in strains lacking Rrp6p. For several substrates, these are distinct from the defects seen in strains mutant for core exosome components or Mtr4p. Comparison of the phenotypes of *rrp47*-Δ, *rrp6*-Δ, and *rrp47*-Δ

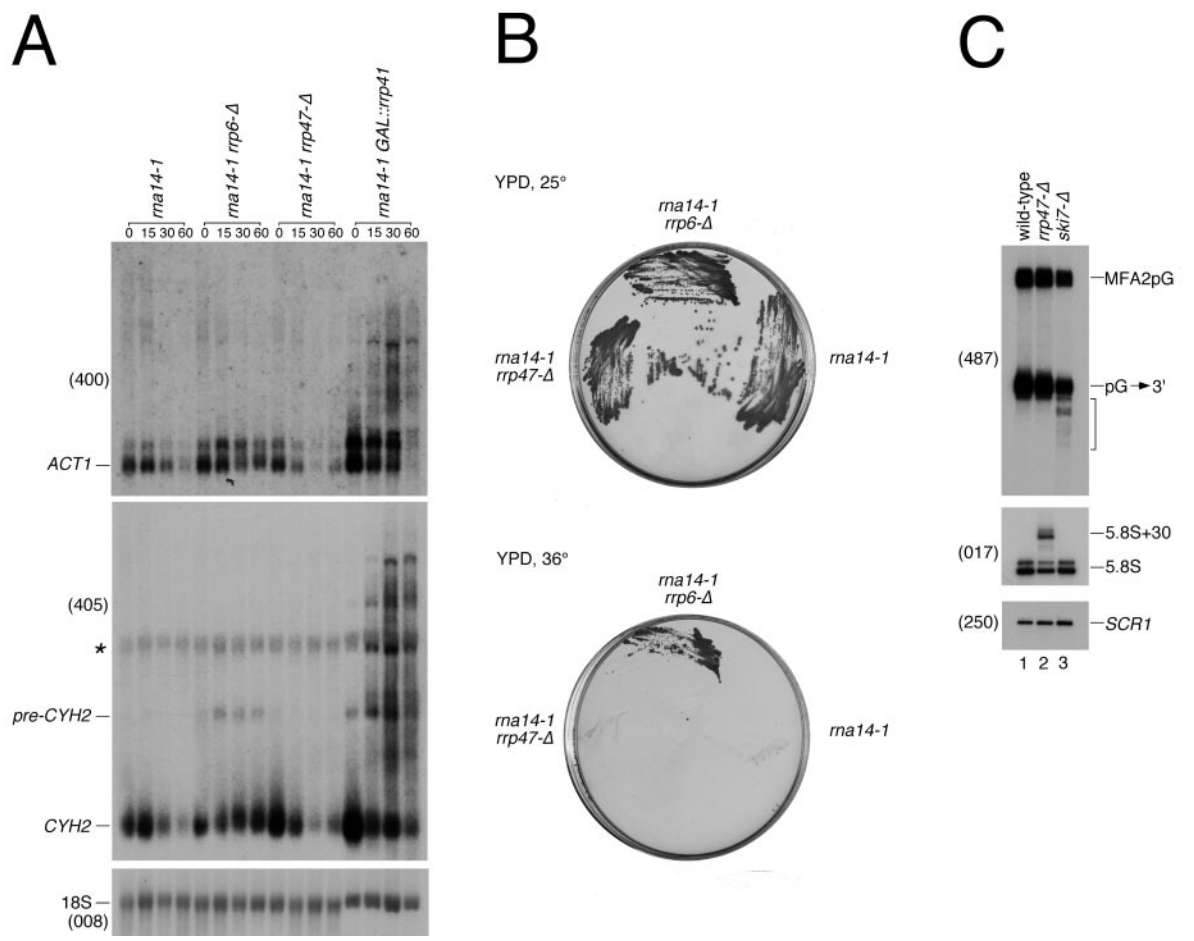

FIG. 7. Rrp47p is not required for nuclear mRNA surveillance or cytoplasmic mRNA decay. (A) Northern blot analysis of RNA isolated from *rna14-1*, *rna14-1 rrp6-*Δ, *rna4-1 rrp47-*Δ, and *rna14-1 GAL::rrp41* mutants during growth at 23°C (zero time points) and after transfer to 37°C for 15, 30, and 60 min. Blots were hybridized with probes specific to *ACT1* and *CYH2* mRNAs and to 18S rRNA as a loading control. A nonspecific RNA detected with the *CYH2* probe is indicated with an asterisk. The probes used are indicated in brackets to the left of each panel. (B) Plate growth assay of the *rna14-1*, *rna14-1 rrp47-*Δ, and *rna14-1 rrp6-*Δ mutants on YPD medium at 25 and 36°C. Plates were incubated for 5 days. (C) Northern blot analysis of RNA from wild-type (lane 1), *rrp47-*Δ (lane 2), and *ski7-*Δ (lane 3) strains expressing the *MFA2pG* reporter transcript. Hybridization was performed with probe 487, complementary to the 3′ end of the poly(G) cassette within the *MFA2* 3′ untranslated region. The probe detects the full-length *MFA2pG* transcript and the poly(G)→3′ fragment (pG→3′). Shortened degradation intermediates of the poly(G)→3′ fragment detectable in the *ski7-*Δ mutant are indicated by a bracket on the right-hand side of the panel. The lower panels show control hybridizations of the same Northern with probes complementary to the 5.8S rRNA (oligonucleotide 017) and the *SCR1* RNA (oligonucleotide 250).

rrp6-Δ double mutants suggested that Rrp47p functions to promote Rrp6p activity. The absence of Rrp47p did not significantly affect either the expression level of Rrp6p or its coimmunoprecipitation with Rrp4p (R. Houalla and D. Tollervey, unpublished observations), suggesting that Rrp47p is not required for Rrp6p expression or its assembly into the exosome. Although Rrp47p shares no similarity with characterized 3′→5′ exoribonucleases, the homologous human protein C1D binds strongly to nucleic acids (28). Rrp47p may therefore function in substrate recruitment and targeting to Rrp6p.

Significantly, the effects of the absence of Rrp47p and Rrp6p, although related, were not identical, and not all nuclear functions of the exosome required Rrp47p. In particular, no effect was observed in the absence of Rrp47p on the exosome-mediated degradation of readthrough transcripts observed in the *rna14-1* mutant, which is defective in pre-mRNA cleavage and transcription termination (7, 42). This indicates that Rrp47p may facilitate interactions between the Rrp6p-exosome complex and specific classes of exosome substrates.

Rrp47p was previously reported to function in DNA double-strand break repair and the homologous human protein C1D binds with high affinity to free 3′ ends of DNA (14, 28). Both nonhomologous end joining and homologous recombination events involve nucleotide removal from the free ends by exonucleases. The RNase D family of 3′→5′ exonucleases, which includes Rrp6p, is closely related to the proofreading domain of RNA polymerases (27). Rrp47p may therefore regulate exonucleolytic activities required for both stable RNA processing and DNA repair.

ACKNOWLEDGMENTS

We thank Jeremy Brown (University of Newcastle, Newcastle, United Kingdom) for plasmid pJE39.

This work was supported by the Wellcome Trust.

REFERENCES

1. **Allmang, C., J. Kufel, G. Chanfreau, P. Mitchell, E. Petfalski, and D. Tollervey.** 1999. Functions of the exosome in rRNA, snoRNA and snRNA synthesis. EMBO J. **18:**5399–5410.
2. **Allmang, C., P. Mitchell, E. Petfalski, and D. Tollervey.** 2000. Degradation of ribosomal RNA precursors by the exosome. Nucleic Acids Res. **28:**1684–1691.
3. **Allmang, C., E. Petfalski, A. Podtelejnikov, M. Mann, D. Tollervey, and P. Mitchell.** 1999. The yeast exosome and human PM-Scl are related complexes of 3′->5′ exonucleases. Genes Dev. **13:**2148–2158.
4. **Bachellerie, J. P., J. Cavaille, and A. Huttenhofer.** 2002. The expanding snoRNA world. Biochimie **84:**775–790.
5. **Baudin, A., O. Ozier-Kalogeropoulos, A. Denouel, F. Lacroute, and C. Cullin.** 1993. A simple and efficient method for direct gene deletion in *Saccharomyces cerevisiae*. Nucleic Acids Res. **21:**3329–3330.
6. **Beltrame, M., and D. Tollervey.** 1992. Identification and functional analysis of two U3 binding sites on yeast pre-rRNA. EMBO J. **11:**1531–1542.
7. **Birse, C. E., L. Minvielle-Sebastia, B. A. Lee, W. Keller, and N. J. Proudfoot.** 1998. Coupling termination of transcription to messenger RNA maturation in yeast. Science **280:**298–301.
8. **Bousquet-Antonelli, C., C. Presutti, and D. Tollervey.** 2000. Identification of a regulated turnover pathway for nuclear pre-mRNA. Cell **102:**765–775.
9. **Briggs, M. W., K. T. D. Burkard, and J. S. Butler.** 1998. Rrp6p, the yeast homologue of the human PM-Scl 100-kDa autoantigen, is essential for efficient 5.8S rRNA 3′ end formation. J. Biol. Chem. **273:**13255–13263.
10. **Brown, J. T., X. Bai, and A. W. Johnson.** 2000. The yeast antiviral proteins Ski2p, Ski3p, and Ski8p exist as a complex in vivo. RNA **6:**449–457.
11. **Burkard, K. T. D., and J. S. Butler.** 2000. A nuclear 3′-5′ exonuclease involved in mRNA degradation interacts with poly(A)-polymerase and the hnRNA protein Npl3p. Mol. Cell. Biol. **20:**604–616.
12. **de la Cruz, J., D. Kressler, D. Tollervey, and P. Linder.** 1998. Dob1p (Mtr4p) is a putative ATP-dependent RNA helicase required for the 3′ end formation of 5.8S rRNA in *Saccharomyces cerevisiae*. EMBO J. **17:**1128–1140.
13. **Dichtl, B., D. Blank, M. Ohnacker, A. Friedlein, D. Roeder, H. Langen, and W. Keller.** 2002. A role for SSU72 in balancing RNA polymerase II transcription elongation and termination. Mol. Cell **10:**1139–1150.
14. **Erdemir, T., B. Bilican, T. Cagatay, C. R. Goding, and U. Yavuzer.** 2002. *Saccharomyces cerevisiae* C1D is implicated in both non-homologous DNA end joining and homologous recombination. Mol. Microbiol. **46:**947–957.
15. **Fatica, A., M. Morlando, and I. Bozzoni.** 2000. Yeast snoRNA accumulation relies on a cleavage-dependent/polyadenylation-independent 3′-processing apparatus. EMBO J. **19:**6218–6229.
16. **Gavin, A.-C., M. Bosche, R. Krause, P. Grandi, M. Marzioch, A. Bauer, J. Schultz, J. M. Rick, A.-M. Michon, C.-M. Cruciat, M. Remor, C. Hofert, M. Schelder, M. Brajenovic, H. Ruffner, A. Merino, K. Klein, M. Hudak, D. Dickson, T. Rudi, V. Gnau, A. Bauch, S. Bastuck, B. Huhse, C. Leutwein, M.-A. Heurtier, R. R. Copley, A. Edelmann, E. Querfurth, V. Rybin, G. Drewes, M. Raida, T. Bouwmeester, P. Bork, B. Seraphin, B. Kuster, G. Neubauer, and G. Superti-Furga.** 2002. Functinal organization of the yeast proteome by systematic analysis of protein complexes. Nature **415:**141–147.
17. **Giaever, G., A. M. Chu, L. Ni, C. Connelly, L. Riles, S. Veronneau, S. Dow, A. Lucau-Danila, K. Anderson, B. Andre, A. P. Arkin, A. Astromoff, M. El-Bakkoury, R. Bangham, R. Benito, S. Brachat, S. Campanaro, M. Curtiss, K. Davis, A. Deutschbauer, K. D. Entian, P. Flaherty, F. Foury, D. J. Garfinkel, M. Gerstein, D. Gotte, U. Guldener, J. H. Hegemann, S. Hempel, Z. Herman, D. F. Jaramillo, D. E. Kelly, S. L. Kelly, P. Kotter, D. LaBonte, D. C. Lamb, N. Lan, H. Liang, H. Liao, L. Liu, C. Luo, M. Lussier, R. Mao, P. Menard, S. L. Ooi, J. L. Revuelta, C. J. Roberts, M. Rose, P. Ross-Macdonald, B. Scherens, G. Schimmack, B. Shafer, D. D. Shoemaker, S. Sookhai-Mahadeo, R. K. Storms, J. N. Strathern, G. Valle, M. Voet, G. Volckaert, C. Y. Wang, T. R. Ward, J. Wilhelmy, E. A. Winzeler, Y. Yang, G. Yen, E. Youngman, K. Yu, H. Bussey, J. D. Boeke, M. Snyder, P. Philippsen, R. W. Davis, and M. Johnston.** 2002. Functional profiling of the *Saccharomyces cerevisiae* genome. Nature **418:**387–391.
18. **Henry, Y., H. Wood, J. P. Morrissey, E. Petfalski, S. Kearsey, and D. Tollervey.** 1994. The 5′ end of yeast 5.8S rRNA is generated by exonucleases from an upstream cleavage site. EMBO J. **13:**2452–2463.
19. **Hilleren, P., T. McCarthy, M. Rosbash, R. Parker, and T. H. Jensen.** 2001. Quality control of mRNA 3′-end processing is linked to the nuclear exosome. Nature **413:**538–542.
20. **Jacobs Anderson, J. S., and R. Parker.** 1998. The 3′ to 5′ degradation of yeast mRNAs is a general mechanism for mRNA turnover that requires the SKI2 DEVH box protein and 3′ to 5′ exonucleases of the exosome complex. EMBO J. **17:**1497–1506.
21. **Kiss, T.** 2002. Small nucleolar RNAs: an abundant group of noncoding RNAs with diverse cellular functions. Cell **109:**145–148.
22. **Kumar, A., S. Agarwal, J. A. Heyman, S. Matson, M. Heidtman, S. Piccirillo, L. Umansky, A. Drawid, R. Jansen, Y. Liu, K. H. Cheung, P. Miller, M. Gerstein, G. S. Roeder, and M. Snyder.** 2002. Subcellular localization of the yeast proteome. Genes Dev. **16:**707–719.
23. **Lafontaine, D., and D. Tollervey.** 1996. One-step PCR mediated strategy for the construction of conditionally expressed and epitope-tagged yeast proteins. Nucleic Acids Res. **24:**3469–3472.
24. **Liang, S., M. Hitomi, Y.-H. Hu, Y. Liu, and A. M. Tartakoff.** 1996. A DEAD-box-family protein is required for nucleocytoplasmic transport of yeast mRNA. Mol. Cell. Biol. **16:**5139–5146.
25. **Mitchell, P.** 2001. Purification of yeast exosome. Methods Enzymol. **342:**356–364.
26. **Mitchell, P., E. Petfalski, A. Shevchenko, M. Mann, and D. Tollervey.** 1997. The exosome: a conserved eukaryotic RNA processing complex containing multiple 3′->5′ exoribonucleases. Cell **91:**457–466.
27. **Moser, M. J., W. R. Holley, A. Chatterjee, and S. Mian.** 1997. The proofreading domain of *Escherichia coli* DNA polymerase I and other DNA and/or RNA exonuclease domains. Nucleic Acids Res. **25:**5110–5118.
28. **Nehls, P., T. Keck, R. Greferath, E. Spiess, T. Glaser, K. Rothbarth, H. Stammer, and D. Werner.** 1998. cDNA cloning, recombinant expression and characterization of polypeptides with exceptional DNA affinity. Nucleic Acids Res. **26:**1160–1166.
29. **Oeffinger, M., A. Lueng, A. I. Lamond, and D. Tollervey.** 2002. Yeast pescadillo is required for multiple activities during 60S ribosomal subunit synthesis. RNA **8:**626–636.
30. **Ooi, S. L., D. A. Samarsky, F. M. J., and J. D. Boeke.** 1998. Intronic snoRNA biosynthesis in *Saccharomyces cerevisiae* depends on the lariat-debranching enzyme: intron length effects and activity of a precursor snoRNA. RNA **4:**1096–1110.
31. **Petfalski, E., T. Dandekar, Y. Henry, and D. Tollervey.** 1998. Processing of the precursors to small nucleolar RNAs and rRNAs requires common components. Mol. Cell. Biol. **18:**1181–1189.
32. **Puig, O., F. Caspary, G. Rigaut, B. Rutz, E. Bouveret, E. Bragado-Nilsson, M. Wilm, and B. Sèraphin.** 2001. The tandem affinity purification (TAP) method: a general procedure of protein complex purification. Methods Enzymol. **24:**218–219.
33. **Rasmussen, T. P., and M. R. Culbertson.** 1998. The putative nucleic acid helicase Sen1p is required for formation and stability of termini and for maximal rates of synthesis and levels of accumulation of small nucleolar RNAs in *Saccharomyces cerevisiae.* Mol. Cell. Biol. **18:**6885–6896.
34. **Schevchenko, A., O. N. Jensen, A. V. Podtelejnikov, F. Sagliocco, M. Wilm, O. Vorm, P. Mortensen, A. Shevchenko, H. Boucherie, and M. Mann.** 1996. Linking genome and proteome by mass spectrometry: large scale identification of yeast proteins from two-dimensional gels. Proc. Natl. Acad. Sci. USA **93:**14440–14445.
35. **Torchet, C., B.-A. C. Milligan, E. Thompson, J. Kufel, and D. Tollervey.** 2002. Processing of 3′-extended read-through transcripts by the exosome can generate functional mRNAs. Mol. Cell **9:**1285–1296.
36. **Tucker, M., and R. Parker.** 2000. Mechanisms and control of mRNA decapping in *Saccharomyces cerevisiae*. Annu. Rev. Biochem. **69:**571–595.
37. **van Hoof, A., P. Lennertz, and R. Parker.** 2000. Yeast exosome mutants accumulate 3′-extended polyadenylated forms of U4 small nuclear RNA and small nucleolar RNAs. Mol. Cell. Biol. **20:**441–452.
38. **van Hoof, A., R. R. Staples, R. E. Baker, and R. Parker.** 2000. Function of the Ski4p (Csl4p) and Ski7p proteins in 3′-to-5′ degradation of mRNA. Mol. Cell. Biol. **20:**8230–8243.
39. **Venema, J., and D. Tollervey.** 1999. Ribosome synthesis in *Saccharomyces cerevisiae*. Annu. Rev. Genet. **33:**261–311.
40. **Venema, J., and D. Tollervey.** 1996. *RRP5* is required for formation of both 18S and 5.8S rRNA in yeast. EMBO J. **15:**5701–5714.
41. **Yavuzer, U., G. C. M. Smith, T. Bliss, D. Werner, and S. P. Jackson.** 1998. DNA end-independent activation of DNA-PK mediated via association with the DNA-binding protein C1D. Genes Dev. **12:**2188–2199.
42. **Yonaha, M., and N. J. Proudfoot.** 2000. Transcriptional termination and coupled polyadenylation in vitro. EMBO J. **19:**3770–3777.
43. **Zanchin, N. I. T., and D. S. Goldfarb.** 1999. The exosome subunit Rrp43p is required for the efficient maturation of 5.8S, 18S, and 25S rRNA. Nucleic Acids Res. **27:**1283–1288.